ELSEVIER

NeuroImage

www.elsevier.com/locate/ynimg
NeuroImage 32 (2006) 1167 – 1175

Technical Note

Anterior cingulate cortex: An MRI-based parcellation method

Laurie M. McCormick,[a,*] Steven Ziebell,[a] Peggy Nopoulos,[a] Martin Cassell,[b] Nancy C. Andreasen,[a,c] and Michael Brumm,[a]

[a]*Department of Psychiatry, University of Iowa, Roy J. and Lucille A. Carver College of Medicine, 200 Hawkins Drive, W268 GH, Iowa City, IA 52242, USA*
[b]*Department of Anatomy and Cell Biology, University of Iowa Hospitals and Clinics, Iowa City, IA 52242, USA*
[c]*The MIND Institute and the University of New Mexico, Albuquerque, NM, New Mexico*

Received 6 December 2005; revised 19 March 2006; accepted 28 April 2006
Available online 20 July 2006

Objective: **The anterior cingulate cortex (ACC) is an important part of the limbic system involved in emotions, cognition and executive function. The ACC has structurally distinct subregions, both microscopically and functionally, that have been implicated in several major psychiatric disorders. However, a structural analysis of these subregions with magnetic resonance imaging (MRI) has not been done. Our main purpose was to develop an MRI-based parcellation method of the ACC that permits us to explore plausible abnormalities in 4 functionally relevant subregions: dorsal, rostral, subcallosal and subgenual.**

Methods: **The reliability study for gray matter volume and surface area of each subregion was performed on 14 randomly selected MR scans by 3 different raters. Our method posits to conserve the topographic uniqueness of individual brains and is based on our ability to visualize both the 3-dimensional rendered brain and the 3 orthogonal planes simultaneously with BRAINS2 software. We developed rules to hand-trace regions of interest (ROI) to surround contiguous areas of gray matter for dorsal, rostral, subcallosal and subgenual regions. The ACC was then parcellated into these 4 distinct subregions (8 when both right and left hemispheres were measured).**

Results and discussion: **The intraclass *R* coefficients for gray matter volume of each subregion ranged between 0.85 and 0.93. The current study describes a new highly reliable and reproducible topography-based parcellation method of the ACC into its dorsal, rostral, subcallosal and subgenual regions.**

Conclusions: **This new parcellation method provides a new means of exploring the role of the functionally and structurally distinct subregions of the ACC in schizophrenia, depression and various other brain illnesses.**

Keywords: Anterior cingulate; ACC; Parcellation method; MRI; Paracingulate

Introduction

The anterior cingulate cortex (ACC) is structurally complex and important in behavioral neuroscience and neuroimaging, yet no studies to date have identified a reliable method to measure the morphology of the functionally distinct subregions of this area. The ACC is one of the largest parts of the limbic system, embedded within the frontal cortex (MacLean, 1990), which coordinates frontal lobe activity with subcortical drive from the basal ganglia (Mega and Cohenour, 1997). It plays a major role in executive cognitive, attention and motor functioning as well as mediating emotions (Devinsky et al., 1995; Paus, 2001; Yucel et al., 2003). Based on lesion and stimulation studies, the ACC has been shown to be associated with personality change, apathy, inattention and even akinetic mutism (Bancaud et al., 1992; Cohen et al., 1999; Nemeth et al., 1988; Tow and Whitty, 1953). These changes have been correlated to changes in regional blood flow and metabolism in the ACC (Bush et al., 2000; Drevets, 1999; George et al., 1995; Mayberg et al., 1999; Skaf et al., 2002).

The ACC contains a number of anatomically and functionally distinct regions (Devinsky et al., 1995; Dum and Strick, 1991; Shima and Tanji, 1998; Vogt et al., 1995). Several lines of evidence from functional imaging and lesion studies suggest a broad division of the ACC into dorsal and ventral areas (Bush et al., 2000; Koski and Paus, 2000; Paus, 2001; Yucel et al., 2003). The dorsal aspect of the ACC has been found to be strongly associated with specific motor, attention and cognitive functions (MacDonald et al., 2000), whereas the ventral aspects of the ACC (rostral, subcallosal and subgenual regions) are involved with emotions, mood and autonomic functions (Mayberg et al., 2002).

There are distinct cytoarchitectural and functional connectivity differences between the dorsal and rostral regions of the ACC (Devinsky et al., 1995; Koski and Paus, 2000). The presence of spindle-shaped neurons within the rostral ACC is a recent evolutionary specialization that is only found in humans and the great apes (Allman et al., 2001; Nimchinsky et al., 1995).

* Corresponding author. Fax: +1 319 353 8656.
E-mail address: laurie-mccormick@uiowa.edu (L.M. McCormick).
Available online on ScienceDirect (www.sciencedirect.com).

1053-8119/$ - see front matter © 2006 Elsevier Inc. All rights reserved.
doi:10.1016/j.neuroimage.2006.04.227

Since severe mental illness appears to be unique to the human condition and it seems to arise from a combination of both environmental stress and genetic predisposition, improved understanding of the structural MRI abnormalities in this region may be important. Indeed, both structural and functional anomalies of the ACC have *also* been described in several major psychiatric syndromes including schizophrenia, depression and obsessive-compulsive disorder (Ashton et al., 2000; Benes, 1993; Sigmundsson et al., 2001; Suhara et al., 2002; Theberge et al., 2003). Antidepressant medication responses can be quantified through functional imaging of the rostral and subgenual regions of the ACC (Drevets et al., 1997; Mayberg et al., 2000). Metabolic and electrical changes in the rostral and subgenual regions of the ACC have been described in depression and even help predict clinical response to antidepressant treatment (Mayberg et al., 2002; Pizzagalli et al., 2001). Similarly, decreased dorsal ACC activity has been found in patients at high risk of developing schizophrenia and can predict who will go on to have the disorder (Morey et al., 2005). Decreased subcallosal ACC activity has also been described in patients with severe depression (Drevets, 1999).

The only volumetric studies on an ACC subregion have been on the subcallosal/subgenual region in patients with mood disorders (Coryell et al., 2005; Drevets et al., 1997). The relevant area in these studies included the ACC immediately ventral to the genu of the corpus callosum and extending to where the putamen is first seen within the basal ganglia. However, this delineation excluded a significant portion of Brodmann's area 25, which has strong anatomical links with the ventral tegmental area, periaqueductal gray, hypothalamus and dorsal medulla (Freedman et al., 2000). The subgenual ACC which includes Brodmann's area 25 is overactive in depression (Mayberg et al., 2002). Suppression of activity in area 25 with continuous electrical stimulation has been shown to alleviate treatment-resistant depression (Mayberg et al., 2005).

There are methods for parcellating the ACC as a whole for imaging purposes (Crespo-Facorro et al., 1999), but there are no established reliable guidelines for parcellating its functionally distinct areas: rostral, dorsal, subgenual and subcallosal. The main purpose of this study was then to develop a reliable magnetic resonance image (MRI)-based parcellation method of the ACC based on reliable topographic landmarks that permits us to explore plausible structural abnormalities in functionally relevant ACC subregions. Our method posits to conserve the topographic uniqueness of individual brains and is based on our ability to visualize both the 3-dimensional rendered brain and the 3 orthogonal planes simultaneously with BRAINS2 software (Magnotta et al., 2002). We developed rules to hand-trace regions of interest (ROI) to surround contiguous areas of gray matter for dorsal, rostral, subcallosal and subgenual regions. The ACC was then reliably parcellated into these 4 distinct subregions (8 when both right and left hemispheres were measured).

Methods

Subjects

A set of 10 MR scans were randomly selected for tracing the ACC regions. An additional 4 scans representing each of the 4 ACC sulcal variations were also included for a total of 14 MR scans. The MRI scans were obtained from a database pool from the University of Iowa Mental Health Clinical Research Center. This included healthy volunteers recruited from the community and individuals diagnosed with schizophrenia. A mixture of subjects was included because the method was developed for application to studies that include both schizophrenia and healthy controls.

MRI acquisition

MR scans were obtained for each subject with a standard T_1-weighted three-dimensional spoiled gradient recall acquisition sequence on a 1.5 T General Electric Signa scanner (GE Medical Systems, Milwaukee, WI) (TE = 5, TR = 24, flip angle = 40°, NEX = 2, FOV = 26, matrix = 256 × 192, 1.5-mm slice thickness). The two-dimensional PD and T_2 sequences were acquired as follows: 3.0 or 4.0 mm thick coronal slices (TE = 36 ms (for PD) and 96 ms (for T_2), TR = 3000 ms, NEX = 1, FOV = 26, matrix = 256 × 192). The in-plane resolution is 1.016 × 1.016 mm for the three modalities.

Image processing

MR data were visually assessed for quality and movement artifacts, and MR scans were repeated if needed. The scans were then processed on Linux workstations with locally developed BRAINS2 software (Magnotta et al., 2002). The T_1-weighted images were spatially normalized and resampled to 1.0 mm^3 voxels so that the anterior–posterior axis of the brain was realigned parallel to the ACPC line and the interhemispheric fissure aligned on the other two axes. The T_2 and PD-weighted images were aligned to the spatially normalized T_1-weighted image (Woods, 1992). The data sets were then segmented using the multispectral data and a discriminate analysis method based on automated training class selection (Harris et al., 1999). The tissue-classified image was then used to generate a triangle-based iso-surface using a threshold of 130 representing pure gray matter, which corresponds to the parametric center of the cortex (Magnotta et al., 1999). This triangulated surface was used as the basis for our calculations of volume.

Rules for defining ACC subregions

The ACC was divided into 4 subregions, dorsal, rostral, subcallosal and subgenual using major landmarks which define three vertical planes, A, B and C (Fig. 1). Plane A defines the posterior end of the rostral ACC, thus separating the latter from the anterior limits of both the dorsal and subcallosal ACC. It is drawn on the coronal plane, one slice forward from the slice in which the two sides of the anterior corpus callosum are no longer connected through the genu (Fig. 7b). Next, plane B defines the posterior boundary of the subcallosal ACC, separating it from the subgenual ACC. Plane B is drawn one coronal slice before the putamen is seen within the basal ganglia (Figs. 9c and 10b). Occasionally, this plane may be drawn separately for the left and right sides depending upon when the putamen is first present on each side. To make this subtle distinction, one has to go back and forth through several slices within this region. Plane C defines the posterior boundary of the dorsal ACC. It is drawn in the sagittal plane as a vertical line through the middle (or tip) of the first gyrus anterior to where the ascending marginal sulcus (ascending ramus) joins the prominent cingulate sulcus (CS) horizontally (Fig. 6a). This plane is drawn between the anterior and posterior commissure

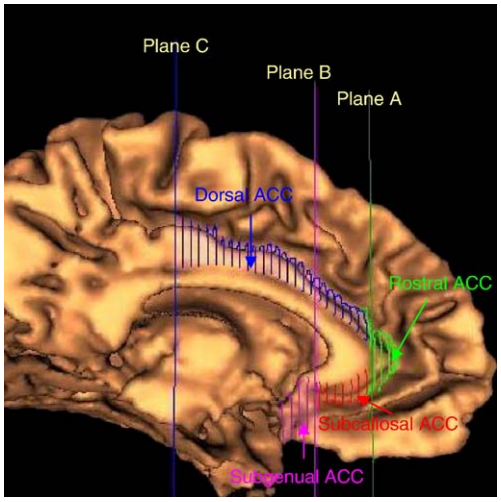

Fig. 1. The ACC is divided into 4 distinct structural and functional subregions by using 3 vertical planes A, B, and C to define: dorsal, rostral, subcallosal, and subgenual subregions of the ACC.

that are automatically generated with BRAINS2 software. This differs from the Crespo-Facorro et al. (1999) method in that their plane is determined by looking at the top of the brain on the axial view and finding the central sulcus and placing the plane there.

The actual tracing of the ACC subregions is then done by creating a region of interest (ROI) on alternating serial coronal slices (every 2.0 mm). The ROI of gray matter is drawn as a circle with a beginning and an end around the cortical surface ribbon (in purple; Fig. 6b). The white matter included in these slices is not included in these analyses. The sagittal, coronal and transaxial slices are also examined to obtain an overall view of the ACC. We also leave the surface view on to help better delineate the boundaries of these subregions.

Since there are considerable variations in the sulcal patterns of the cingulate between individuals on the macroscopic level (Caviness et al., 1999; Ono et al., 1990; Yucel et al., 2002), we examined and photographed 34 post-mortem brains to fully assess the large variations in the cingulate and paracingulate gyri that have been described of this area. We have identified 4 examples of these variations. The first example is a single anterior cingulate

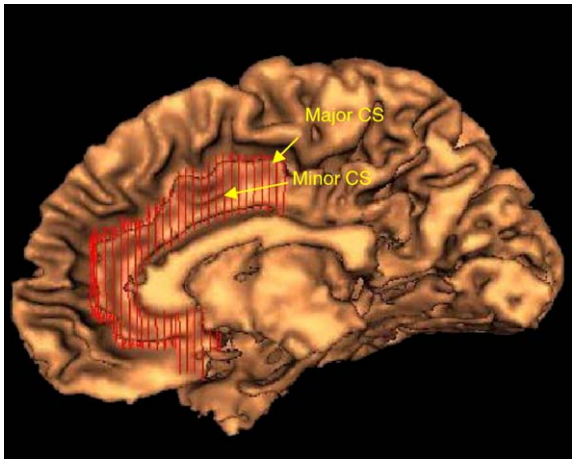

Fig. 2. The first ACC variation is a minor secondary sulcus in the dorsal ACC.

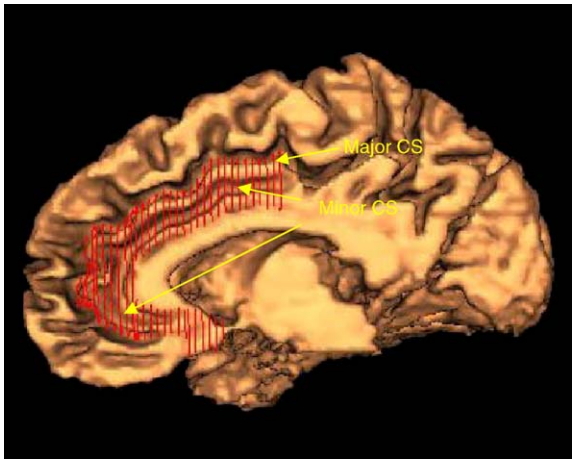

Fig. 3. The second ACC variation is a double cingulate throughout the dorsal, rostral, and subcallosal subregions.

with a minor secondary sulcus in the dorsal region (Fig. 2). In this first example, the secondary minor sulcus may or may not be present at plane C. The second example is double cingulate with a secondary sulcus present throughout the dorsal, rostral and subcallosal regions (Fig. 3). Here, the secondary sulcus is present at plane C and is deeper and thus considered the major sulcus. The third example is of a second cingulate that starts within the dorsal region and becomes the prominent cingulate within the rostral and ventral ACC regions (Fig. 4). This switch occurs when the secondary CS becomes the deepest sulcus, which may or may not be more superior than the slice at plane C. The secondary cingulate may also not be present until the rostral region, but continues as the main cingulate within the subcallosal area. The fourth example is of a secondary cingulate that emerges within the dorsal region of the ACC anterior to plane C but disappears as the primary cingulate continues on in the rostral and subcallosal regions (Fig. 5).

The rule for distinguishing a true second cingulate from a paracingulate gyrus relates to whether the second CS becomes the deepest sulcus within the dorsal or rostral region when viewed on the coronal view. Otherwise, the secondary or external gyrus is

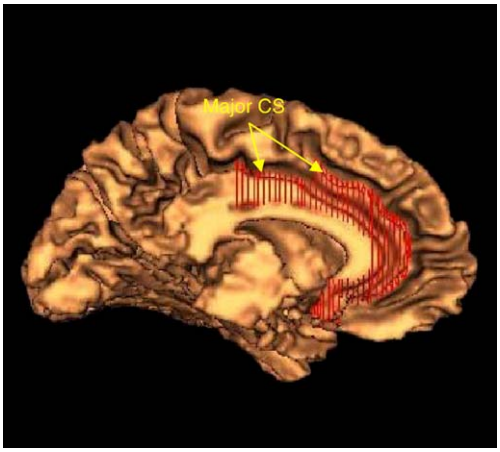

Fig. 4. The third ACC variation is a secondary minor cingulate that starts in the mid-dorsal ACC region and becomes the prominate cingulate cortex within the rostral and subcallosal/subgenual ACC regions as the primary cingulate cortex dissapears.

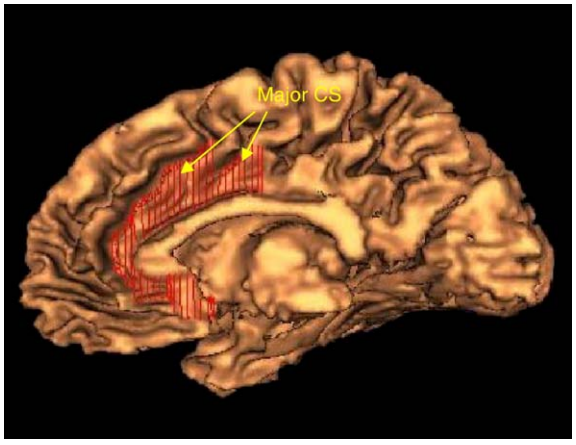

Fig. 5. The fourth ACC variation is a secondary minor cingulate that starts in the dorsal ACC region and dissapears as the primary cingulate cortex continues in the rostral and subcallosal/subgenual ACC regions.

considered to be a paracingulate sulcus and is not included as part of the ACC. Whenever a secondary cingulate sulcus emerges within the dorsal or rostral region as the deepest sulcus, the transition is often gradual for several slices. When tracing this transition area, it is important to look at the surface view to ensure a smooth ROI tracing of the area. Additionally, a second cingulate is often only present on one side of the brain.

Dorsal ACC

We always start with placement of plane C to define the posterior boundary of the dorsal ACC and to separate the posterior cingulate cortex from the ACC. Plane C is drawn in the sagittal plane as a vertical line through the middle (or tip) of the first gyrus anterior to where the ascending marginal sulcus (ascending ramus) joins the prominent CS horizontally (Fig. 6a). This junction corresponds closely to the cytoarchitectural boundary between anterior cingulate area 24 and posterior cingulate area 23 (Vogt et al., 1995). The dorsal ACC is traced on alternating coronal slices starting at plane C and moving anteriorly forward. The left and right sides are parcellated separately on the coronal view. The left side of the dorsal ACC is usually bigger than the right. The anterior margin of the dorsal ACC is then delineated as 1 slice posterior to plane A drawn vertically at the rostral edge of the genu of the corpus callosum, i.e. where the portions of the corpus callosum in each hemisphere are no longer connected. The deepest point of the callosal sulcus and the deepest point of the cingulate sulcus constitute the inferior and superior inner and the outer boundary of the ACC in each coronal slice, respectively (see Figs. 6b–c). Using these criteria, the dorsal ACC corresponds very closely to area 24′ of Vogt (1992, 1995).

Rostral ACC

The posterior margin of the rostral ACC starts at plane A (Fig. 7a). Plane A is placed where the forceps minor of the corpus callosum is no longer connected through the genu on the coronal view (Fig. 7b). The rostral ACC is then traced on alternating coronal slices. The anterior boundary occurs when the cingulate gyrus is no longer present anterior for each side (Figs. 7c–d). Often, the anterior-most boundary of the rostral ACC ends at a different point for each side. If there is a double CS present rostrally, the boundary is determined on the coronal slice where the

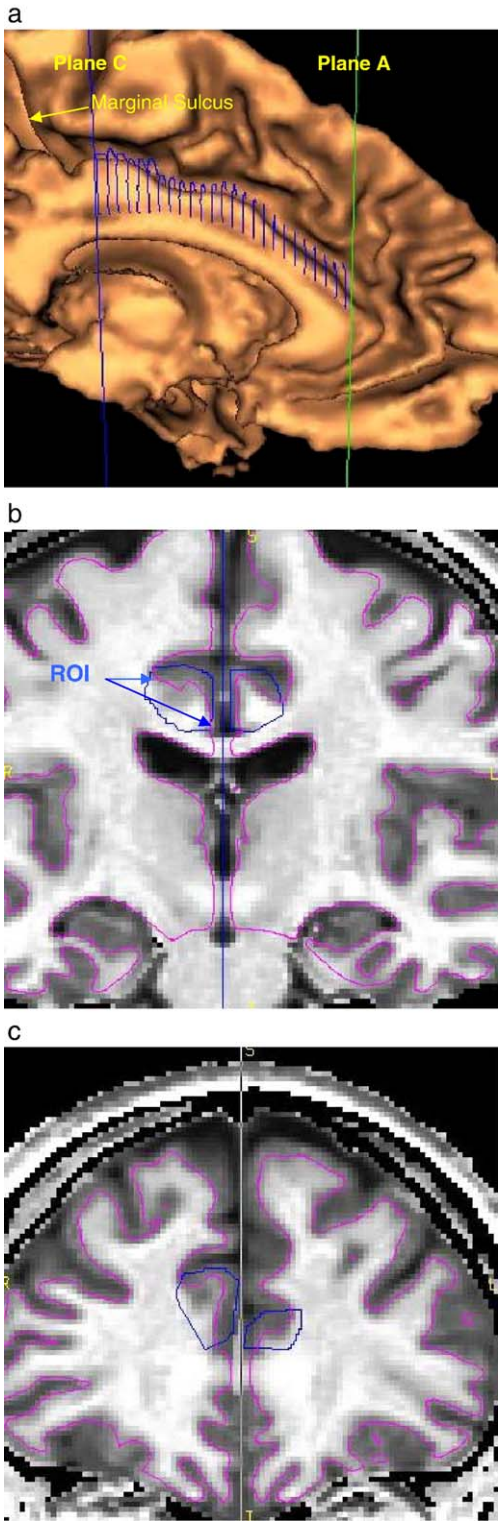

Fig. 6. Parcellation scheme for the dorsal ACC. (a) The dorsal ACC is separated from the posterior cingulate cortex by plane C and by the rostral ACC by plane A. Plane C is drawn in the saggital plane as a vertical line through the tip of the first gyrus anterior to the where the ascending ramus becomes horizontal, while plane A is drawn one slice forward past where the two sides of the corpus callosum are no longer connected through the genu; (b) the ROI for the dorsal ACC is then traced separately on the left and right sides, on alternating coronal slices from the deepest point of the callosal sulcus and the deepest point of the cingulate sulcus moving forward anteriorly from plane C; (c) it is traced until 1 slice posterior of plane A.

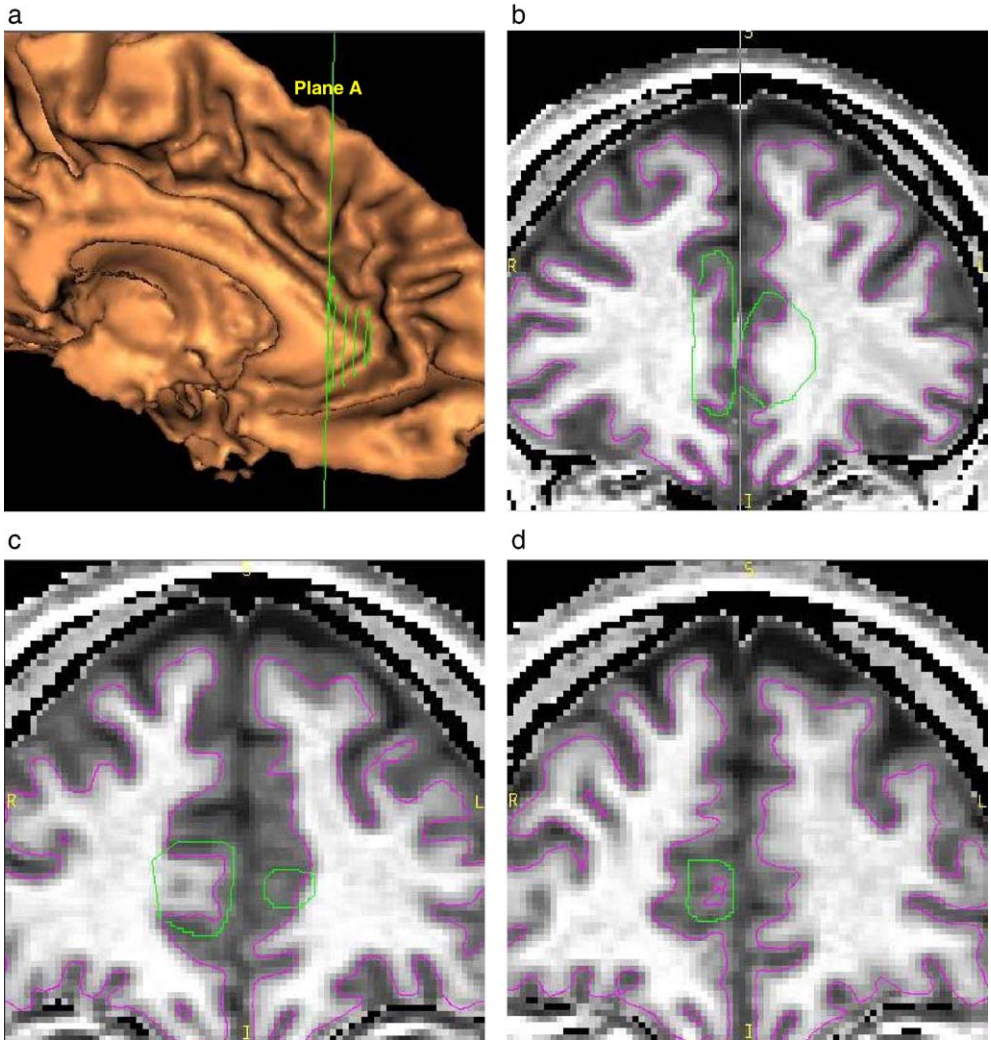

Fig. 7. Parcellation scheme for the rostral ACC. (a) The rostral ACC is separated from the dorsal ACC by plane A. (b) Plane A is drawn one slice forward past where the two sides of the corpus callosum are no longer connected through the genu, best visualized on the coronal plane; (c) it is also traced from the deepest point of the callosal sulcus and the deepest ponit of the cingulate sulcus on alternating coronal slices until the cingulate gryus is no longer present on each side at its most anterior point, (d) in this example, the left side is present 2 slices anterior to the right.

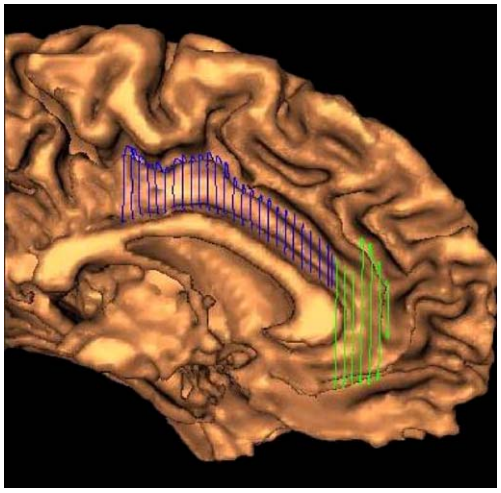

Fig. 8. The rostral ACC may contain a double cingulate in which case the surface view can help approximate the border of this region when the deepest sulcus of the double cingulate (determined on the coronal view) extends beyond the natural C shape of the ACC.

deepest sulcus is present (Fig. 8). The superior frontal gyrus should not be included, which is best determined on the surface view. The rostral ACC thus defined corresponds topographically to areas 24a, 24b and 24c of Vogt et al. (1995) and others. Occasionally, there may be a protrusion of the anterior portion of the rostral ACC in which case tracing the ROI should approximate the normal C-shape of the ACC (best determined on the surface view). When a bridging gyrus is present, the superior boundary of the rostral ACC is best determined on the coronal slices by the deepest sulcus that binds the dorsal and rostral ACC.

Subcallosal ACC

The subcallosal region always includes only the continuation of the rostral cingulate gyrus (areas 24a and 24b) wrapping around the corpus callosum (Fig. 9a). A secondary gyrus may be included only if the secondary sulcus is the deepest sulcus seen on the coronal plane as long as the secondary gyrus is not actually the medial frontal cortex (see Crespo-Facorro et al., 1999). When the deepest sulcus ventral to the corpus callosum includes the medial frontal cortex, the inferior boundary of the subcallosal ACC (the

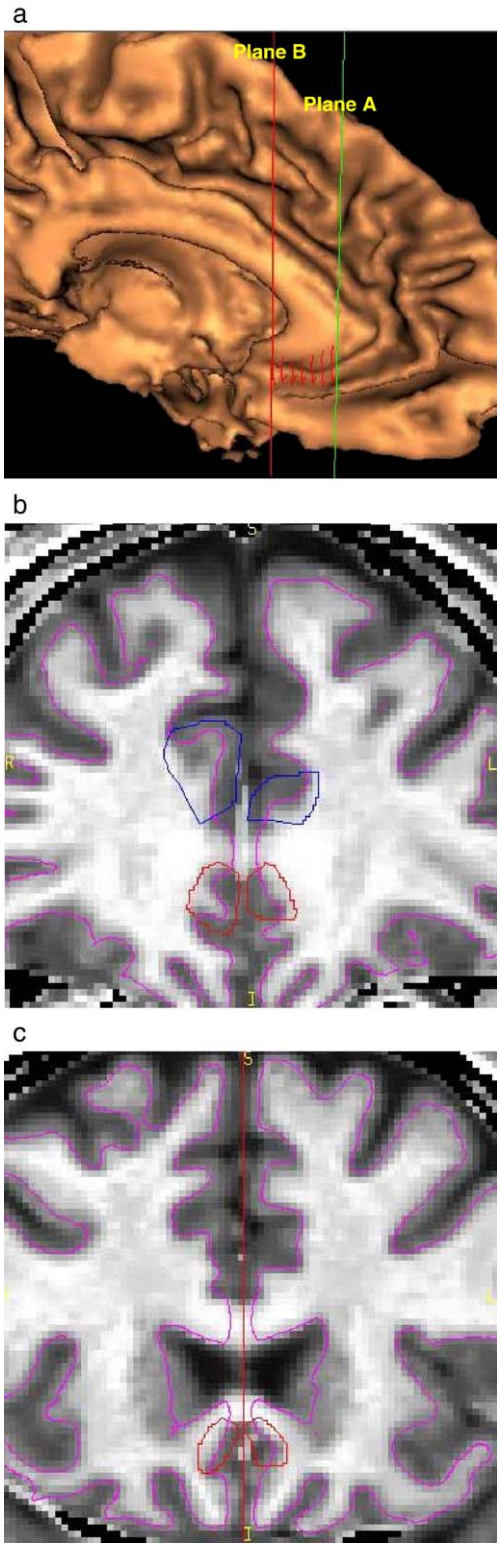

Fig. 9. Parcellation scheme of the subcallosal ACC. (a) The subcallosal ACC is an extension of the ACC ventrally and is separated anteriorly from the rostral ACC by plane A and posteriorly from the subgenual ACC by plane B. Plane B is drawn one slice posterior to where the putamen is first visualized within the basal ganglia; (b) the ROI for the subcallosal ACC is then traced separately for the left and right sides on alternating coronal slices moving forward posteriorly from plane A; (c) and extends to plane B.

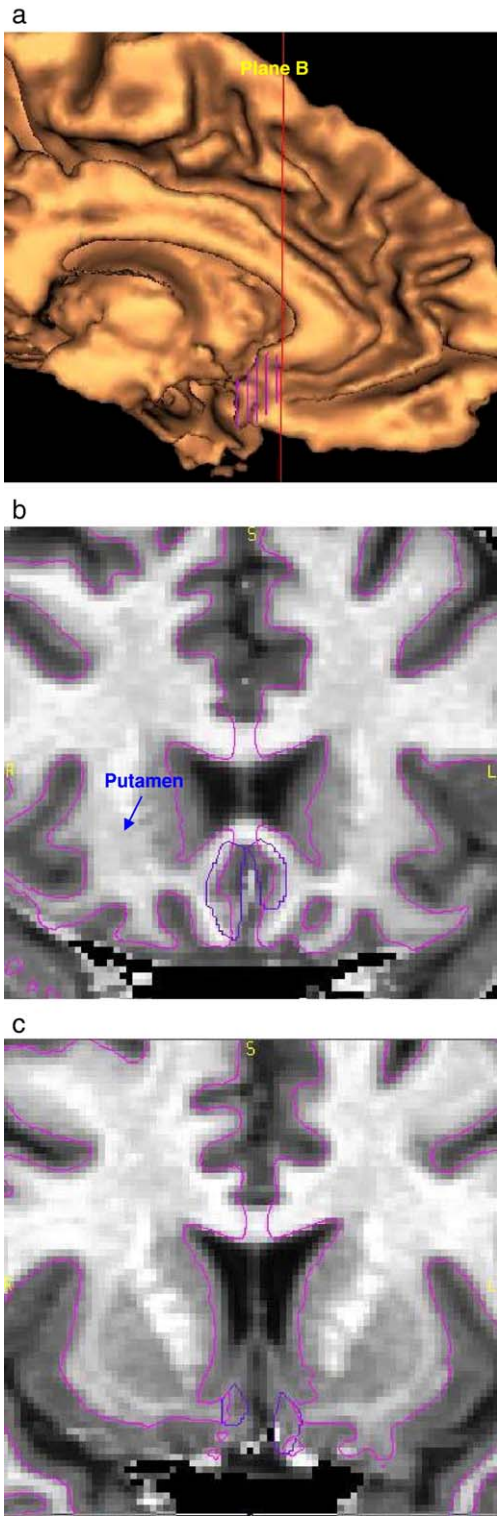

Fig. 10. Parcellation scheme of the subcallosal ACC. (a) The subgenual ACC is separated anteriorly from the subcallosal ACC by plane B. (b) The first slice of the subgenual ACC ROI is drawn one slice posterior to plane B where the putamen is first visualized within the basal ganglia; (c) the ROI for this region is also traced on every coronal slice from the deepest point of the callosal sulcus and the deepest ponit of the cingulate sulcus until the cingulate gryus is no longer present on each side at its most posterior point.

Table 1
ACC regional volumes (cc) for each tracer and the differences between the three tracers

ACC subregions	Right hemisphere mean (SD)				Left hemisphere mean (SD)			
	Tracer 1	Tracer 2	Tracer 3	Differences	Tracer 1	Tracer 2	Tracer 3	Differences
Dorsal	4.33 (0.94)	4.47 (0.89)	4.02 (0.82)	0.95 (0.40)	3.61 (0.62)	3.61 (0.64)	3.53 (0.50)	0.07 (0.93)
Rostral	3.15 (1.14)	2.93 (1.00)	3.05 (1.24)	0.12 (0.88)	2.08 (0.87)	1.80 (0.75)	2.07 (0.87)	0.51 (0.60)
Subcallosal	0.71 (0.17)	0.66 (0.20)	0.59 (0.19)	1.45 (0.25)	0.64 (0.24)	0.63 (0.27)	0.60 (0.22)	0.13 (0.88)
Subgenual	0.67 (0.17)	0.66 (0.17)	0.70 (0.19)	0.16 (0.86)	0.67 (0.20)	0.65 (0.22)	0.71 (0.20)	0.29 (0.75)

ACC = anterior cingulate cortex; SD = standard deviation.

ventral CS) is actually defined by a smaller sulcus. This inferior boundary should also be continuous with the ventral portion of the rostral ACC. The superior boundary is defined at the margin where the gray matter intersects with the white matter of the corpus callosum. The anterior margin of the subcallosal ACC is drawn on the coronal view, one slice behind plane A. This is also the slice defining the anterior border of the dorsal ACC (Fig. 9b). The posterior boundary is drawn at plane B on the coronal plane, which is one slice anterior to where the putamen first becomes present within the basal ganglia (Fig. 9c).

Subgenual ACC

The subgenual region is a posterior continuation of the subcallosal region but usually expands into a vertically oriented gyrus, the paraterminal gyrus, before merging into the caudal end of the gyrus rectus and the anterior perforated substance (Fig. 10a). Brodmann (1909) and most subsequent authors (e.g. Vogt and Vogt, 1919; Rose, 1928; Sarkissov et al., 1955) placed area 25 or its equivalent in the paraterminal gyrus. As with the subcallosal ACC, the superior boundary is defined at the margin where gray matter intersects with white matter of the corpus callosum. The anterior margin of the subgenual ACC starts where the putamen is first seen within the basal ganglia, one slice behind plane B (Fig. 10b). This corresponds well with the point of transition between the horizontally oriented subcallosal continuation of the cingulate gyrus and the beginning of the more vertical cytoarchitectural area of the paraterminal gyrus (e.g. Vogt and Vogt, 1919; Rose, 1928). The posterior boundary is drawn on the coronal plane where the paraterminal gyrus disappears medially (Fig. 10c). The inferior boundary is located at the tip of the lower-most gyrus on the medial surface. This overlaps (or at least merges) with the Crespo-Facorro et al. (1999)—defined straight gyrus (aka gyrus rectus). Often, this inferior border is not continuous with the inferior boundary of the subcallosal ACC and instead merges with the straight gyrus. As with the anterior border of the rostral ACC, both the anterior and posterior border of the subgenual ACC may differ between the two hemispheres. We suggest that this smaller region of the ACC actually be traced on every slice rather than every other one as with the other regions.

Reliability

BRAINS2 software was used to visualize 2D slices of the brain with surface, coronal and sagittal views. Three raters (S.Z., L.M. and M.B.) traced the subregions within the ACC using all of these views to guide parcellation within the specified landmarks discussed above. Before the reliability study began, two of the raters worked on several brains for setting all the conventions and anatomical landmarks that had been utilized for methodological development in order to reduce the legitimate differences in anatomical judgments by raters. The set of brains on which the raters "practiced" was entirely different from the set of brains on which the reliability study was done. A unique set of 14 brains was used to trace each of the ACC subregions. These included brains that have at least one side with 1 of the 4 major sulcal variations. The mean cortical gray matter volume (cm^3) and surface area (mm^2) measurements of each ACC and the mean differences between the three tracers are shown in Tables 1 and 2, respectively.

Inter-rater reliability for all subregions was calculated with intraclass *R* coefficients for cortical gray matter volume and surface area measurements (Table 3). The lowest reliability was in the right subgenual ACC surface at 0.77, while the highest reliability was 0.94 in the right subcallosal ACC surface.

Discussion

The current study describes a new highly reliable and reproducible topography-based parcellation method for subdividing the ACC into 4 subregions: dorsal, rostral, subcallosal and subgenual. This method was developed for two purposes: to provide a quantitative assessment of cortical surface and gray matter volume in reliable anatomical regions using MRI and to provide functionally relevant ROIs in coregistered functional MRI, positron emission tomography and electroencephalography studies. We have drawn on the strengths of the existing method of Crespo-Facorro et al. (1999) but made adaptations and

Table 2
ACC regional surface (mm^2) for each tracer and the differences between the three tracers

ACC subregions	Right hemisphere mean (SD)				Left hemisphere mean (SD)			
	Tracer 1	Tracer 2	Tracer 3	Differences	Tracer 1	Tracer 2	Tracer 3	Differences
Dorsal	1110.69 (195.31)	1152.58 (203.44)	1160.79 (230.65)	0.95 (0.40)	1029.44 (144.09)	991.85 (164.57)	979.82 (153.61)	0.07 (0.93)
Rostral	715.30 (282.17)	635.57 (230.41)	699.84 (276.66)	0.12 (0.88)	470.63 (185.20)	421.96 (177.98)	448.42 (185.31)	0.18 (0.84)
Subcallosal	160.43 (56.84)	165.65 (56.43)	173.55 (60.74)	1.45 (0.25)	183.83 (58.50)	183.93 (66.47)	187.84 (56.62)	1.34 (0.88)
Subgenual	177.95 (37.19)	150.82 (34.02)	154.74 (39.65)	0.16 (0.89)	141.58 (55.07)	126.20 (49.29)	126.34 (54.28)	0.29 (0.75)

ACC = anterior cingulate cortex; SD = standard deviation.

Table 3
Intraclass *R* coefficients for gray matter volumes of 4 ACC subregions in a sample of 14 brains by three raters

ACC subregions	Intraclass *R*			
	Volume		Surface	
	Right	Left	Right	Left
Dorsal	0.85	0.91	0.89	0.87
Rostral	0.89	0.86	0.90	0.87
Subcallosal	0.88	0.93	0.94	0.92
Subgenual	0.85	0.86	0.77	0.88

ACC = anterior cingulate cortex; R = regression.

improvements. We found that the previous method for defining plane A left significant variation between raters and that the rules for including paracingulate gyri were also quite variable. We have defined plane B as the point at where the putamen is first seen within the basal ganglia to incorporate the same boundaries of the subcallosal ACC that is used by Drevets (personal communication). This is different than the plane B used by Crespo-Facorro et al. (1999). Instead, our plane B separates the ventral aspect of the ACC into subcallosal and subgenual regions, whereas plane A located more anteriorly, divides the rostral and dorsal regions of the ACC at a point where the corpus callosum is no longer connected. We have also incorporated Brodmann's area 25, previously left out of previous ACC parcellation methods, into our subgenual region. In our sample of normal controls and patients with schizophrenia, we did not find any obvious or identifiable differences in the subcortical and cortical landmarks that would cause regional volume differences.

We have made every effort to incorporate the microscopically defined borders of Brodmann's areas 24 and 25 described by Devinsky et al. (1995) into this MRI parcellation method. The superior cingulate gyrus or paracingulate gyrus was included in previous parcellation method of Crespo-Facorro et al. (1999). A second cingulate or paracingulate gyrus may be present in about 35–40% of individuals (Ono et al., 1990; Paus et al., 1996; Vogt et al., 1995). Due to the fact that there is such large variability in paracingulate and double cingulate sulci (Paus et al., 1996), we defined our posterior plane (plane C) by the first gyrus intersection with the primary CS. We did not include the paracingulate gyrus in our parcellation method because it represents Brodmann's area 32 (e.g. Vogt et al., 1995). However, we did account for variations in the presence of a double cingulate within the ACC proper (see Figs. 4 and 6). Thus, we developed these reliable conventions to reduce interobserver differences in anatomical judgments and feel that we developed more stringent guidelines for including the entire ACC, as well as the large variations that occur primarily in the dorsal and rostral portions of the ACC and for reliably dividing the functionally relevant subregions of the ACC.

The major disadvantage of this method is that it is still somewhat time-consuming as it takes about 30 min to parcellate each brain. Since the subcallosal and subgenual ACC volumes are relatively small areas, small errors in parcellating the regions can be exaggerated. Thus, reliability needs to be established for each rater prior to individual parcellation projects. In the future, an automated method to conduct parcellation of these ACC subregions may be available. Furthermore, probability maps in Talairach space would represent an important refinement of our method.

The ACC parcellation method presented here uses a landmark (the putamen) outside of the region of interest. Our anatomical analysis of post-mortem brains (see also Paus et al., 1996), for which we report 4 variant patterns, suggests that the cingulate sulcal patterns are not consistent enough to use as internal landmarks. We believe that an easily recognizable external reference point such as the putamen probably introduces less variability in defining subregions of the ACC than relying on local sulci. Furthermore, subcallosal volumetric studies using the methods developed by Drevets et al. (1997) also use the putamen as the anterior boundary of this region. Alternative landmarks, such as the internal genu of the corpus callosum, could be used to demarcate the anterior boundary of the subcallosal ACC.

In conclusion, we have presented here a reliable topography-based MRI parcellation method of the frontal lobe that will allow us to use a new approach in understanding the role of separate ACC subregions in the pathophysiology of psychosis and other brain illnesses. Since structural neuroimaging studies have failed to provide a clear picture of ACC abnormalities in schizophrenia, we felt that a more thorough approach to the anatomy of this region was needed. We hope that this method will help clarify the existence of subtle gross structural abnormalities in the specific subregions of the ACC that might reflect underlying neuropathological processes in schizophrenia and other illnesses. We hope that a more accurate parcellation system of the ACC will help improve the spatial resolution of coregistering functional imaging studies with structural volume differences in these subregions.

Acknowledgments

Support: This project was funded by NIH grants: MH43271, MH31593, MH40856.

References

Allman, J.M., Hakeem, A., Erwin, J.M., Nimchinsky, E., Hof, P., 2001. The anterior cingulate cortex. The evolution of an interface between emotion and cognition. Ann. N. Y. Acad. Sci. 935, 107–117.

Ashton, L., Barnes, A., Livingston, M., Wyper, D., 2000. Cingulate abnormalities associated with PANSS negative scores in first episode schizophrenia. Behav. Neurol. 12 (1–2), 93–101.

Bancaud, J., Talairach, J., Caviness, Jr., V.S., Lange, N.T., Makris, N., Herbert, M.R., Kennedy, D.N., Cohen, R.A., Kaplan, R.F., Moser, D.J., Jenkins, M.A., Wilkinson, H., 1992. Clinical semiology of frontal lobe seizures. Adv. Neurol. 57, 3–58.

Benes, F.M., 1993. Neurobiological investigations in cingulate cortex of schizophrenic brain. Schizophr. Bull. 19 (3), 537–549.

Brodmann K., 1909. Vergleichende Lokalisationslehre der Großhirnrinde in ihren Prinzipien dargestellt auf Grund des Zellenbaues. Leipzig: Barth JA.

Bush, G., Luu, P., Posner, M.I., 2000. Cognitive and emotional influences in anterior cingulate cortex. Trends Cogn. Sci. 4 (6), 215–222.

Caviness, Jr., V.S., Lange, N.T., Makris, N., Herbert, M.R., Kennedy, D.N., 1999. MRI-based brain volumetrics: emergence of a developmental brain science. Brain Dev. 21 (5), 289–295.

Cohen, R.A., Kaplan, R.F., Moser, D.J., Jenkins, M.A., Wilkinson, H., 1999. Impairments of attention after cingulotomy. Neurology 53 (4), 819–824.

Coryell, W., Nopoulos, P., Drevets, W., Wilson, T., Andreasen, N.C., 2005. Subgenual prefrontal cortex volumes in major depressive disorder and

schizophrenia: diagnostic specificity and prognostic implications. Am. J. Psychiatry 162 (9), 1706–1712.
Crespo-Facorro, B., Kim, J.J., Andreasen, N.C., O'Leary, D.S., Wiser, A.K., Bailey, J.M., Harris, G., Magnotta, V.A., 1999. Human frontal cortex: an MRI-based parcellation method. NeuroImage 10 (5), 500–519.
Devinsky, O., Morrell, M.J., Vogt, B.A., 1995. Contributions of anterior cingulate cortex to behaviour. Brain 118 (Pt. 1), 279–306.
Drevets, W.C., 1999. Prefrontal cortical–amygdalar metabolism in major depression. Ann. N. Y. Acad. Sci. 877, 614–637.
Drevets, W.C., Price, J.L., Simpson, Jr., J.R., Todd, R.D., Reich, T., Vannier, M., Raichle, M.E., 1997. Subgenual prefrontal cortex abnormalities in mood disorders. Nature 386 (6627), 824–827.
Dum, R.P., Strick, P.L., 1991. The origin of corticospinal projections from the premotor areas in the frontal lobe. J. Neurosci. 11 (3), 667–689.
Freedman, L.J., Insel, T.R., Smith, Y., 2000. Subcortical projections of area 25 (subgenual cortex) of the macaque monkey. J Comp. Neurol. 421 (2), 172–188.
George, M.S., Ketter, T.A., Parekh, P.I., Horwitz, B., Herscovitch, P., Post, R.M., 1995. Brain activity during transient sadness and happiness in healthy women. Am. J. Psychiatry 152 (3), 341–351.
Harris, G., Andreasen, N.C., Cizadlo, T., Bailey, J.M., Bockholt, H.J., Magnotta, V.A., Arndt, S., 1999. Improving tissue classification in MRI: a three-dimensional multispectral discriminant analysis method with automated training class selection. J. Comput. Assist. Tomogr. 23 (1), 144–154.
Koski, L., Paus, T., 2000. Functional connectivity of the anterior cingulate cortex within the human frontal lobe: a brain-mapping meta-analysis. Exp. Brain. Res. 133 (1), 55–65.
MacDonald, III, A.W., Cohen, J.D., Stenger, V.A., Carter, C.S., 2000. Dissociating the role of the dorsolateral prefrontal and anterior cingulate cortex in cognitive control. Science 288 (5472), 1835–1838.
MacLean, P.D., 1990. The Triune Brain in Evolution: Role in Paleocerebral Functions. Plenum Press, New York.
Magnotta, V.A., Heckel, D., Andreasen, N.C., Cizadlo, T., Corson, P.W., Ehrhardt, J.C., Yuh, W.T., 1999. Measurement of brain structures with artificial neural networks: two- and three-dimensional applications. Radiology 211 (3), 781–790.
Magnotta, V.A., Harris, G., Andreasen, N.C., O'Leary, D.S., Yuh, W.T., Heckel, D., 2002. Structural MR image processing using the BRAINS2 toolbox. Comput. Med. Imaging Graph. 26 (4), 251–264.
Mayberg, H.S., Liotti, M., Brannan, S.K., McGinnis, S., Mahurin, R.K., Jerabek, P.A., Silva, J.A., Tekell, J.L., Martin, C.C., Lancaster, J.L., Fox, P.T., 1999. Reciprocal limbic–cortical function and negative mood: converging PET findings in depression and normal sadness. Am. J. Psychiatry 156 (5), 675–682.
Mayberg, H.S., Brannan, S.K., Tekell, J.L., Silva, J.A., Mahurin, R.K., McGinnis, S., Jerabek, P.A., 2000. Regional metabolic effects of fluoxetine in major depression: serial changes and relationship to clinical response. Biol. Psychiatry 48 (8), 830–843.
Mayberg, H.S., Silva, J.A., Brannan, S.K., Tekell, J.L., Mahurin, R.K., McGinnis, S., Jerabek, P.A., 2002. The functional neuroanatomy of the placebo effect. Am. J. Psychiatry 159 (5), 728–737.
Mayberg, H.S., Lozano, A.M., Voon, V., McNeely, H.E., Seminowicz, D., Hamani, C., Schwalb, J.M., Kennedy, S.H., 2005. Deep brain stimulation for treatment-resistant depression. Neuron 45 (5), 651–660.
Mega, M.S., Cohenour, R.C., 1997. Akinetic mutism: disconnection of frontal–subcortical circuits. Neuropsychiatry Neuropsychol. Behav. Neurol. 10 (4), 254–259.
Morey, R.A., Inan, S., Mitchell, T.V., Perkins, D.O., Lieberman, J.A., Belger, A., 2005. Imaging frontostriatal function in ultra-high-risk, early, and chronic schizophrenia during executive processing. Arch. Gen. Psychiatry 62 (3), 254–262.
Nemeth, G., Hegedus, K., Molnar, L., 1988. Akinetic mutism associated with bicingular lesions: clinicopathological and functional anatomical correlates. Eur. Arch. Psychiatry Neurol. Sci. 237 (4), 218–222.
Nimchinsky, E.A., Vogt, B.A., Morrison, J.H., Hof, P.R., 1995. Spindle neurons of the human anterior cingulate cortex. J. Comp. Neurol. 355 (1), 27–37.
Ono, M., Kubik, S., Abernathey, C.D., 1990. Atlas of the Cerebral Sulci. Georg Thieme Verlag, New York.
Paus, T., 2001. Primate anterior cingulate cortex: where motor control, drive and cognition interface. Nat. Rev., Neurosci. 2 (6), 417–424.
Paus, T., Tomaiuolo, F., Otaky, N., MacDonald, D., Petrides, M., Atlas, J., Morris, R., Evans, A.C., 1996. Human cingulate and paracingulate sulci: pattern, variability, asymmetry, and probabilistic map. Cereb. Cortex 6 (2), 207–214.
Pizzagalli, D., Pascual-Marqui, R.D., Nitschke, J.B., Oakes, T.R., Larson, C.L., Abercrombie, H.C., Schaefer, S.M., Koger, J.V., Benca, R.M., Davidson, R.J., 2001. Anterior cingulate activity as a predictor of degree of treatment response in major depression: evidence from brain electrical tomography analysis. Am. J. Psychiatry 158 (3), 405–415.
Rose, M., 1928. Die Inserlinde des Menschen und der Tiere. J. Psychol. Neurol. 37, 467–624.
Sarkissov, S.A., Filimonoff, I.N., Kononowa, E.P., Preobraschenskaja, I.S., Kukuew, L.A., 1955. Atlas of the Cytoarchitectonics of the Human Cerebral Cortex. Medgiz, Moscow.
Shima, K., Tanji, J., 1998. Role for cingulate motor area cells in voluntary movement selection based on reward. Science 282 (5392), 1335–1338.
Sigmundsson, T., Suckling, J., Maier, M., Williams, S., Bullmore, E., Greenwood, K., Fukuda, R., Ron, M., Toone, B., 2001. Structural abnormalities in frontal, temporal, and limbic regions and interconnecting white matter tracts in schizophrenic patients with prominent negative symptoms. Am. J. Psychiatry 158 (2), 234–243.
Skaf, C.R., Yamada, A., Garrido, G.E., Buchpiguel, C.A., Akamine, S., Castro, C.C., Busatto, G.F., 2002. Psychotic symptoms in major depressive disorder are associated with reduced regional cerebral blood flow in the subgenual anterior cingulate cortex: a voxel-based single photon emission computed tomography (SPECT) study. J. Affect. Disord. 68 (2–3), 295–305.
Suhara, T., Okubo, Y., Yasuno, F., Sudo, Y., Inoue, M., Ichimiya, T., Nakashima, Y., Nakayama, K., Tanada, S., Suzuki, K., Halldin, C., Farde, L., 2002. Decreased dopamine D2 receptor binding in the anterior cingulate cortex in schizophrenia. Arch. Gen. Psychiatry 59 (1), 25–30.
Theberge, J., Al-Semaan, Y., Williamson, P.C., Menon, R.S., Neufeld, R.W., Rajakumar, N., Schaefer, B., Densmore, M., Drost, D.J., 2003. Glutamate and glutamine in the anterior cingulate and thalamus of medicated patients with chronic schizophrenia and healthy comparison subjects measured with 4.0-T proton MRS. Am. J. Psychiatry 160 (12), 2231–2233.
Tow, P.M., Whitty, C.W., 1953. Personality changes after operations on the cingulate gyrus in man. J. Neurochem. 16 (3), 186–193.
Vogt, C., Vogt, O., 1919. Allgemeinere ergbnisse unserer Hirnforschung. J. Psychol. Neurol. 25, 399–462.
Vogt, B.A., Finch, D.M., Olson, C.R., 1992. Functional heterogeneity in cingulate cortex: the anterior executive and posterior evaluative regions. Cereb. Cortex 2 (6), 435–443.
Vogt, B.A., Nimchinsky, E.A., Vogt, L.J., Hof, P.R., 1995. Human cingulate cortex: surface features, flat maps, and cytoarchitecture. J. Comp. Neurol. 359 (3), 490–506.
Woods, S.W., 1992. Regional cerebral blood flow imaging with SPECT in psychiatric disease: focus on schizophrenia, anxiety disorders, and substance abuse. J. Clin. Psychiatry 53, 20–25 (Suppl.)
Yucel, M., Stuart, G.W., Maruff, P., Wood, S.J., Savage, G.R., Smith, D.J., Crowe, S.F., Copolov, D.L., Velakoulis, D., Pantelis, C., 2002. Paracingulate morphologic differences in males with established schizophrenia: a magnetic resonance imaging morphometric study. Biol. Psychiatry 52 (1), 15–23.
Yucel, M., Wood, S.J., Fornito, A., Riffkin, J., Velakoulis, D., Pantelis, C., 2003. Anterior cingulate dysfunction: implications for psychiatric disorders? J. Psychiatry Neurosci. 28 (5), 350–354.